

Parametric Resonances in Axionic Cosmic Strings

Jose J. Blanco-Pillado^{1,2,3*}, Daniel Jiménez-Aguilar^{1,2†},
Jose M. Queiruga^{4,5‡} and Jon Urrestilla^{1,2 §}

¹ *Department of Physics, University of Basque Country, UPV/EHU, 48080, Bilbao, Spain*

² *EHU Quantum Center, University of Basque Country, UPV/EHU*

³ *IKERBASQUE, Basque Foundation for Science, 48011, Bilbao, Spain*

⁴ *Department of Applied Mathematics,*

University of Salamanca, 37008, Salamanca, Spain

⁵ *Institute of Fundamental Physics and Mathematics,*

University of Salamanca, 37008 Salamanca, Spain.

Abstract

In this letter we uncover a new parametric resonance of axionic cosmic strings. This process is triggered by the presence on the string of internal mode excitations that resonantly amplify the amplitude of transverse displacements of the string. We study this process by running numerical simulations that demonstrate the existence of this phenomenon in a $(3+1)$ dimensional lattice field theory and compare the results with the analytic expectations for the effective Lagrangian of the amplitude of these modes and their interactions. Finally, we also analyze the massless and massive radiation produced by these excited strings and comment on its relevance for the interpretation of the results of current numerical simulations of axionic cosmic string networks.

* josejuan.blanco@ehu.eus

† daniel.jimenez@ehu.eus

‡ xose.queiruga@usal.es

§ jon.urrestilla@ehu.eus

I. INTRODUCTION

The nature of dark matter remains as one of the biggest puzzles in cosmology. Among the multiple hypothetical particles that have been proposed as dark matter candidates, the axion is perhaps one of the most promising ones. Particle physics models with axions appear in many well motivated extensions of the Standard Model where an extra $U(1)$ symmetry (the so-called Peccei-Quinn symmetry [1]) is added. This symmetry is broken at high energies leading to the appearance of a Goldstone mode. Eventually, this mode becomes massive due to small instanton contributions at low energies. It is therefore clear that these models lead to the prediction of a new particle with very weak interactions, in other words, a perfect candidate for dark matter [2–6].

In a cosmological context, one can assume that the Peccei-Quinn symmetry is spontaneously broken before inflation. This would lead to an axionic abundance today that depends on the value of the axion field in our local patch of the universe. We will not consider these models in this paper any further. On the other hand, if this symmetry is broken after inflation, the phase transition would lead to the formation of axionic cosmic strings [7–9]. This cosmological network of strings will evolve in an expanding universe producing a spectrum of Goldstone modes. This process will continue until the axion acquires its mass, leading to the formation of domain walls attached to the strings. These walls will typically trigger the annihilation of the string network, a process that will also contribute to the axionic abundance ¹.

It is clear from this description that in order to estimate the relic abundance of axions in these models one needs to have a good understanding of the evolution of this network of axionic strings. This task has been tackled by several groups over the years [11–27]. However, the results of the different groups are not all consistent with one another. One of the issues that is currently under scrutiny is the large scale properties of the network, in particular the density of strings in the so-called *scaling regime*. This is, of course, a key element of the network that directly affects the estimate of the axion abundance in the model.

Another important ingredient needed to compute the cosmological density of axions today is the spectrum of Goldstone mode radiation produced by strings. This spectrum has also been estimated by several groups using different techniques, although a quantitative agreement between different groups has not been reached yet. In this paper, we would like to describe a phenomenon that may have some relevance in the dynamics of axionic cosmic

¹ The cosmological scenario after the walls are formed strongly depends on the details of the axion potential [10].

strings and in turn in the spectrum of the radiation they produce.

As we mentioned above, these axionic cosmic strings appear as solitonic objects in a field theory model with a $U(1)$ global symmetry. The study of small perturbations around the simplest straight string configuration demonstrates the existence of two different types of possible excitations of these objects. The lowest energy excitations correspond to the transverse displacements of the strings. These perturbations can be viewed as massless modes on the $1+1$ dimensional worldsheet of the string and describe wiggles that propagate at the speed of light. Apart from these perturbations, there is another type of excitations that have to do with the internal dynamics of the soliton. These modes appear generically in many field theory models with solitons [28–34]. Physically, they represent the possible deformations of the shape of the relaxed soliton, which means that their masses are typically similar to the energy scale associated to the size of the soliton. However, an interesting aspect of these states is their long lifetime [33–35], which could make them relevant for the long term dynamics of cosmological defects.

The dynamics of global strings has been extensively studied in the literature within the thin wall approximation [9, 36–41]. However, this effective action does not take into account the presence of these massive internal modes of the string. Here we would like to consider the effect that the presence of both types of excitations can have on strings. In particular, we will show that an internal mode excitation could trigger the resonant amplification of the transverse motion of the string. This, in turn, could also accelerate the decay process for the extra energy stored in the string. This is an analogous mechanism to the one recently discovered in domain wall strings in [42].

The organization of the rest of the paper is the following. In section II we discuss the field theory model that we will consider as well as the properties of the linear perturbations around the relaxed axionic string. In section III we study an effective Lagrangian that describes the coupling between these modes and investigate the possible appearance of parametric resonances. In section IV we show how these resonances are easily activated in lattice field theory simulations and compare the results with the analytic predictions obtained in the previous section. Finally, we end with some conclusions about the possible relevance of these findings to the results obtained in field theory simulations of cosmic string networks.

II. AXIONIC STRINGS AND THEIR EXCITATIONS

We will consider the following model for a complex scalar field with a $U(1)_{PQ}$ invariant action of the form

$$S = \int d^4x \left[\partial_\mu \phi^* \partial^\mu \phi - \frac{\lambda}{4} (\phi^* \phi - \eta^2)^2 \right], \quad (1)$$

where λ describes the quartic coupling of the field and η denotes the energy scale of the theory. The form of the potential leads to a symmetry breaking where the vacuum manifold is parametrized by the configurations with $|\phi(x)| = \eta$. The spectrum of fluctuations around these vacua is composed of a massive (radial) field whose mass is $m_r = \sqrt{\lambda}\eta$ and a massless Goldstone mode that represents the perturbations in the field angular phase. The equations of motion obtained from the Lagrangian are

$$\partial_\mu \partial^\mu \phi + \frac{\lambda}{2} (\phi^* \phi - \eta^2) \phi = 0 . \quad (2)$$

Since the first homotopy group of the vacuum manifold is non-trivial, we will look for static string-like solitonic solutions of the form

$$\phi_v(x) = \eta f(\rho) e^{i\theta} , \quad (3)$$

where we have used the cylindrical coordinates (ρ, θ) to parametrize the plane transverse to the string. With this ansatz, one can find the equation of motion for the profile function $f(r)$, namely

$$\frac{d^2 f}{dr^2} + \frac{1}{r} \frac{df}{dr} - \frac{1}{r^2} f - \frac{1}{2} (f^2 - 1) f = 0 , \quad (4)$$

where we have introduced the dimensionless radial coordinate $r = m_r \rho$. The solution of this equation describes a solitonic object with an inner region with $f(r) \approx c r + \dots$ where the field is close to the top of the potential; and an asymptotic region where the field approaches the vacuum as $f(r) \approx 1 - (1/r^2) + \mathcal{O}(1/r^4)$ (see [34] for more details on this solution).

It is important to realize that this solution has a transverse energy density that falls slowly with the distance from the core. This leads to a logarithmic divergence for the energy per unit length of the string. This is a manifestation of another important point. These strings are charged with respect to the Goldstone mode of the theory, and this divergence is just an indication of this fact. Incorporating this coupling to the effective theory of the string means that one should not only take into account the Nambu-Goto action, but also consider the contribution of the Kalb-Rammond term [43].

This divergence does not present a difficulty cosmologically since its contribution is always cut-off by the presence of another string at some distance R from the original string. This leads to an energy per unit length of the form

$$\mu(R) \approx \mu_{\text{core}} + 2\pi\eta^2 \log\left(\frac{R}{\delta}\right) , \quad (5)$$

where δ describes a measure of the size of the inner core of the solution. In a lattice field theory simulation for a string network, the distance between the strings is obviously much smaller than in a realistic cosmological setting. This could have an important effect on the dynamics of these strings, leading, for example, to transient effects in the simulations.

A. String excitations

Let us now consider the possible perturbations around the static straight axionic string presented earlier. In order to study these fluctuations, we take the ansatz

$$\phi(\mathbf{x}, t) = \phi_v(\mathbf{x}) + \delta\phi(\mathbf{x}) \cos(\omega t) . \quad (6)$$

We can now decompose the perturbations in waves along the longitudinal direction of the string, the z direction, of the form

$$\delta\phi(\mathbf{x}) = A \delta\phi(r, \theta) \cos(\omega_z z) . \quad (7)$$

This decomposition leads to a linear system of equations that formally looks like a Schrödinger equation for the function $\delta\phi(r, \theta)$ in a radial potential whose eigenvalue is given by the combination $\omega^2 - \omega_z^2$. This eigenvalue problem is identical to the linear equations for perturbations of the $2d$ vortex, which has been recently studied in detail in [34]. We can use the results obtained in that paper to identify the lowest energy states of these fluctuations in the $3 + 1$ string configuration.

We first note that there are zero mode solutions of these equations with $\omega^2 - \omega_z^2 = 0$. These modes correspond to travelling waves moving at the speed of light along the longitudinal direction of the string. Physically, they represent the Goldstone modes describing the fact that the static string breaks the translational invariance of the theory. When promoted to $3 + 1$ dimensions, these wiggles can be viewed as zero mass excitations on the string worldsheet.

These zero modes are easy to compute since they are just given by the derivative of the static solution along a direction perpendicular to the string. In particular, we have

$$\eta_x^0(r, \theta) \equiv \partial_x \phi_v(\mathbf{x}) \quad \text{and} \quad \eta_y^0(r, \theta) \equiv \partial_y \phi_v(\mathbf{x}) . \quad (8)$$

Note that this zero mode is not normalizable. However, this is just another manifestation of the slow decline of the energy density of the global strings. One can, in fact, find an exact solution of the non-linear equations of motion that represents an arbitrary transverse wiggle moving at the speed of light [44]. These zero modes are therefore the linear approximation of those exact solutions.

Furthermore, it was shown in [34] that this eigenvalue problem possesses an infinite number of bound states in the radial part of the scalar field. These bound states can be found numerically and they represent certain deformations of the internal shape of the vortex. In particular, the first two such modes were obtained numerically in [34]. Here we just reproduce in Fig. 1 the first mode $\delta\phi(r, \theta) = \eta_s(r)e^{i\theta}$, which will be the focus of our

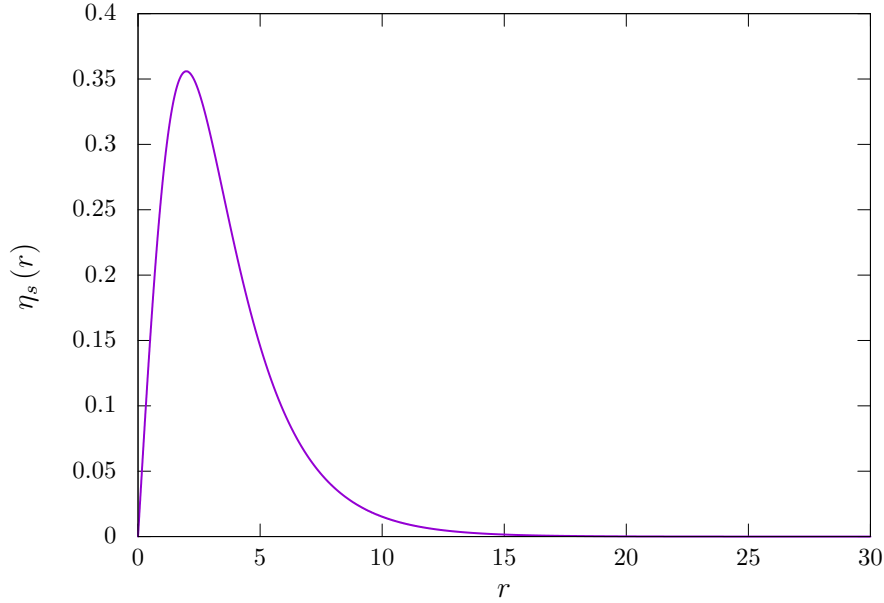


FIG. 1: Bound state function for the first massive mode.

study. The eigenvalue in this case was found to be $w_s^2 \equiv w^2 - w_z^2 = 0.8133$ in units of the square of the mass m_r .

Finally, apart from these bound states we have the continuous scattering states that correspond to the perturbative fluctuations that propagate in the vacuum. These are the massless Goldstone modes that represent fluctuations on the phase of the scalar field and the massive radial excitations whose mass starts at $m = 1$ in these units.

As it was shown in [34], an excited vortex state given by a small amplitude of the *shape mode*, $\eta_s(r)$, could take a long time to decay to its ground state. The reason for this is that its frequency is below the mass threshold for radial modes to propagate in the vacuum. This does not mean, however, that this state is stable since non-linear interactions allow this energy to slowly leak to infinity. This phenomenon can be directly translated to our $(3 + 1)$ configuration by considering a homogenous excitation of the shape mode along the string. The invariance along the z direction of this configuration allows us to use the results from the $2 + 1$ problem.

The situation becomes more interesting in $(3 + 1)$ dimensions due to the non-linear interaction between the different excitations on the string. As we will see in the next sections, we will encounter several types of resonances in the system of interacting modes.

III. PARAMETRIC RESONANCES

Let us now consider the situation of a straight axionic string uniformly excited with the presence of a shape mode. As we described earlier, this mode will couple non-linearly to radiation that slowly leaks this extra energy to infinity in the direction perpendicular to the string. This was already studied in [34]. Here we will be interested in studying the coupling between the shape mode and the transverse wiggle excitations of the string. With this idea in mind, we consider a possible excitation of the string of the form

$$\phi(t, \mathbf{x}) = f(r)e^{i\theta} + A(t)\eta_s(r)e^{i\theta} + D(t)\eta_x^0(r, \theta) \cos(w_z z), \quad (9)$$

where $A(t)$ denotes the amplitude of the shape mode and we take $D(t)$ to represent the amplitude of a standing wave of the displacement of the string along the x direction^{2,3}. We can now insert this ansatz in our action in Eq. (1) to obtain, after integrating along the spatial directions, an effective Lagrangian of the form

$$L_{\text{effec}} = -\mu(R)L_z + 2\pi\eta^2 L_z \left[\dot{A}^2 - w_s^2 A^2 - I_{A,3} A^3 - I_{A,4} A^4 \right. \\ \left. + I_D(R)\dot{D}^2 - (I_{D,2} + I_D(R)w_z^2)D^2 - I_{D,4}D^4 \right. \\ \left. - I_{AD,3} AD^2 - I_{AD,4} A^2 D^2 \right], \quad (10)$$

where the coefficients $I_{A,3}$, $I_{A,4}$, $I_{D,2}$ and $I_{D,4}$ are computed by performing the integrals specified in the Appendix A and represent the finite higher order couplings between these amplitudes. On the other hand, the coefficient $I_D(R)$ can be shown to be logarithmically divergent with the cutoff that we implemented at large distances, namely the distance R .

The equations of motion we obtain from this effective Lagrangian are given by

$$\ddot{A}(t) + (w_s^2 + I_{AD,4} D(t)^2) A(t) + \frac{3}{2}I_{A,3}A(t)^2 + 2I_{A,4}A(t)^3 + \frac{1}{2}I_{AD,3}D(t)^2 = 0, \\ \ddot{D}(t) + \left(w_z^2 + \frac{I_{D,2}}{I_D(R)} + \frac{I_{AD,3}}{I_D(R)}A(t) + \frac{I_{AD,4}}{I_D(R)}A(t)^2 \right) D(t) + 2\frac{I_{D,4}}{I_D(R)}D(t)^3 = 0. \quad (11)$$

At the lowest order, these equations recover the information about the shape and zero modes that we already discussed in the study of the linear regime⁴. Going beyond the linear

² Note that this ansatz disregards completely the presence of any radiation field. This is of course an approximation. Taking this into consideration would become important when we compare the results of our numerical simulations with the predictions of this ansatz.

³ Note that this effective model can be easily extended to describe displacements in the xy plane taking into account that any zero mode perturbation of the string can be expressed as a linear combination of the zero modes in the x, y directions.

⁴ Note, however, that the zero mode acquires a small mass term due to a finite cutoff scale R . Taking the limit of $R \rightarrow \infty$, this term will vanish.

order, we identify the presence of resonance effects between these two modes. Let us start by looking at the zero mode equation. Disregarding the higher order coupling, we get an equation of the form

$$\ddot{D}(t) + \left(w_z^2 + \frac{I_{D,2}}{I_D(R)} + \frac{I_{AD,3}}{I_D(R)} A(t) \right) D(t) = 0 . \quad (12)$$

Assuming the unperturbed shape mode time dependence, namely $A(t) \propto \cos(w_s t)$, we immediately notice that the form of the equation for the displacement of the string is of the Mathieu type [45]. This means that we should expect a parametric resonance behaviour of the string zero mode in the presence of a shape mode excitation. Furthermore, using the information about the different bands of instability of the generic Mathieu equation, we can compute the condition for the zero mode wavelength where we should expect the resonant amplification. This condition can be shown to be

$$\sqrt{w_z^2 + \frac{I_{D,2}}{I_D(R)}} = \frac{w_s}{2} . \quad (13)$$

On the other hand, in situations where the amplitude of the shape mode is small, its equation of motion becomes

$$\ddot{A}(t) + w_s^2 A(t) + \frac{1}{2} I_{AD,3} D(t)^2 = 0 , \quad (14)$$

so we also find a possible source of resonance in case of an oscillating zero mode in $D(t)$. This means that one can also transfer energy resonantly from the zero mode to the internal shape mode, but only when the string oscillates at a frequency comparable to w_s .

This analysis indicates that there are resonant effects in the interaction between these modes. However, we do not expect any runaway process since higher order terms will tame any dramatic behaviour. In reality, we expect to have a transfer of energy between these modes back and forth.⁵ This, however, will have an effect on the amount of radiation emitted from the string which is not taken into account in this effective Lagrangian. We will comment more on this in the next section.

IV. NUMERICAL SIMULATIONS

The analysis presented in the previous section suggests that a uniform excitation of the shape mode on a string will induce a parametric excitation of a zero mode of a particu-

⁵ This was indeed already observed in a similar situation in another field theory model of solitons in 2 + 1 dimensions in [42].

lar wavelength. In this section we show this is indeed the case by running a lattice field simulation of our model.⁶

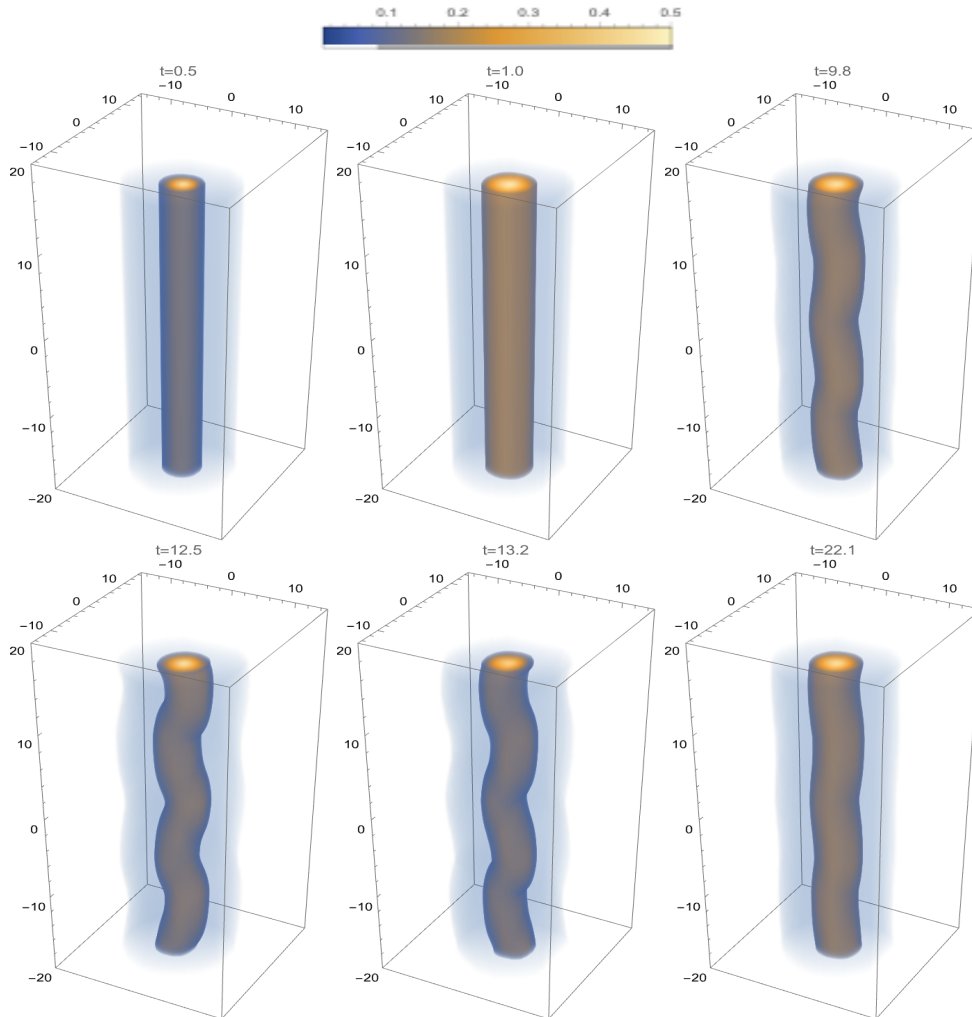


FIG. 2: Evolution of the string energy density in field theory. The initial state corresponds to an excited state with $A(t = 0) = 0.5$ and $D(t = 0) = 0.01$. Top panel, left-to-right, $t = 0.5, 1.0$ and 9.8 . Bottom panel, left-to-right $t = 12.5, 13.2$ and 22.1 . The color palette indicates energy density in units of $\lambda\eta^4$.

We show in Fig. 2 a few snapshots of the position of the string extracted from our field theory simulation starting from an excited state with a shape mode with amplitude $A(t = 0) = 0.5$. We notice how an initially straight string develops a modulation whose amplitude grows for a while before it starts decreasing again⁷. This is exactly what the

⁶ We move the details of the implementation of this numerical simulation to Appendix B.

⁷ In order to accelerate this process in our simulations we give the string a tiny small initial modulation along the x axis to break the symmetry. We have also performed numerical experiments where we place

analytic system of equations given in the previous section predicts. The initial growth is representative of the parametric resonant effect of the Mathieu type equation for the amplitude of the zero mode in the presence of the internal excitation, namely Eq. (12). This behaviour is however cut-off by the presence of non-linear interaction terms in the system of equations. In order to further test the analytic system, we extract the amplitude of both the shape and zero mode directly from the simulation. We can easily do that by projecting the solution onto those modes at any moment in time.⁸ Following this procedure, we can obtain Fig. 3, where we compare the predictions of the system of equations given in Eqs. (11) with the amplitudes of the different modes in the field theory simulation. We note that the solution of the analytic equations is very sensitive to the numerical values of the coefficients. We have found that in order to have a perfect agreement with the results of our simulations we need to slightly modify the numerical coefficients obtained for this setup. We believe this is due to the inaccuracies in the calculation of the coefficients due to numerical error in the functions involved in these calculations (see Appendix A).

Using these coefficients we see a very good agreement with the theoretical expectation for the first oscillation. The subsequent slight deviation is also to be expected since the field theory simulation allows for the presence of radiation from the string, something that is not included in our analytic treatment.

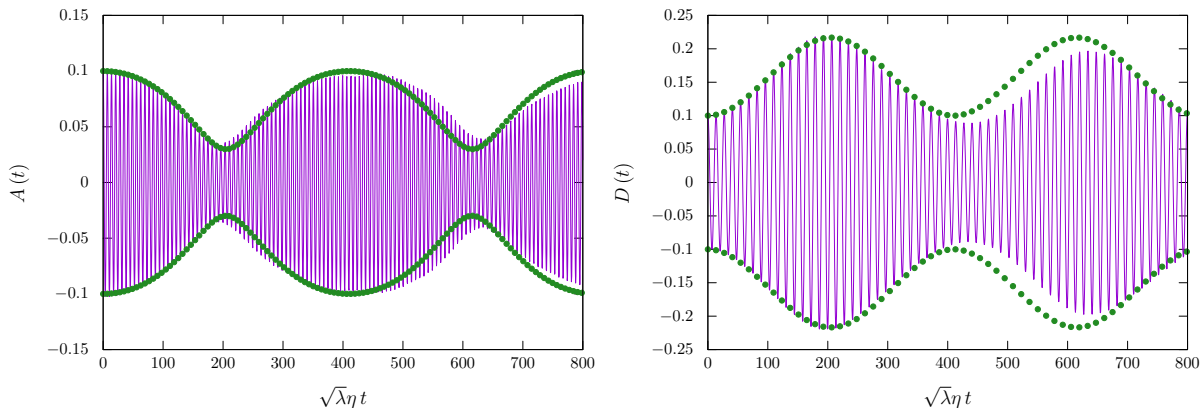


FIG. 3: We show the comparison of the measurements of the shape mode (left) and zero mode (right) from the field theory simulation (in purple) with the results predicted using the equations of motion of our effective Lagrangian (green).

the string in the presence of small random perturbations. This random initial state also triggers the onset of the instability although it takes a longer time to appear.

⁸ We show how this is done in Appendix B.

A. Radiation from the excited string

As we explained in the previous sections, an axionic string is coupled to the massless Goldstone mode that propagates in the vacuum. This can be easily seen if one excites a zero mode on the string. The initial amplitude of this excitation will decrease as the string oscillates mainly due to massless radiation. This has been studied in the literature [9, 37, 39, 40], more notably recently with the aid of adaptive mesh refinement techniques in [41, 46]. We have also performed this type of simulations and obtained a similar result. Most of the energy emitted from an initial zero mode excitation occurs in the form of massless modes assuming a low amplitude regime. Increasing the amplitude of these oscillations, one encounters a mix of massive and massless radiation due to non-perturbative radiative processes similar to the ones observed in other analogous situations in other soliton models (see for example [42, 47]).

On the other hand, a string excited with a homogeneous shape mode perturbation will decay mostly in terms of massive radiation. This was demonstrated in the context of $2 + 1$ dimensional vortices in [34], where we were able to obtain an analytic description of the slow decrease of the amplitude of this mode as a function of time. We have corroborated that this is the case in our current $(3 + 1)$ d setup in cases where there is no instability.

The situation becomes more interesting in the presence of the parametric resonance we discussed earlier. The initial excitation of the shape mode leads to massive radiation due to the coupling of this mode to the massive scattering states. However, the subsequent amplification of the zero mode leads to the appearance of a contribution of massless radiation. The non-linear coupling of the shape and zero modes and their oscillating amplitudes give rise to a complicated pattern of mixed radiation of both modes, massless and massive radiation. We show in Fig. 4 the different contributions of the total energy radiated by the string. We compute this by integrating in time the power of each contribution going through a surface at a large distance from the string.⁹

Finally, we notice that the total energy radiated from the string is increased in the presence of a resonance. This means that the energy stored in the initial internal excitation is radiated away faster than one would have previously estimated from the $2 + 1$ calculation [34]. We show this effect in Fig. 5 by comparing the extra energy in the simulation box for an excited string where the resonant amplification is allowed versus the case where this possibility is prohibited by a small z direction. We see clearly that the presence of the zero mode excitation and the massless radiation deplete the energy of the system faster. This is not surprising since, as we mentioned, this excitation opens up a new channel for decay by

⁹ See the detailed description of the expression of the power computed from the simulation in Appendix B.

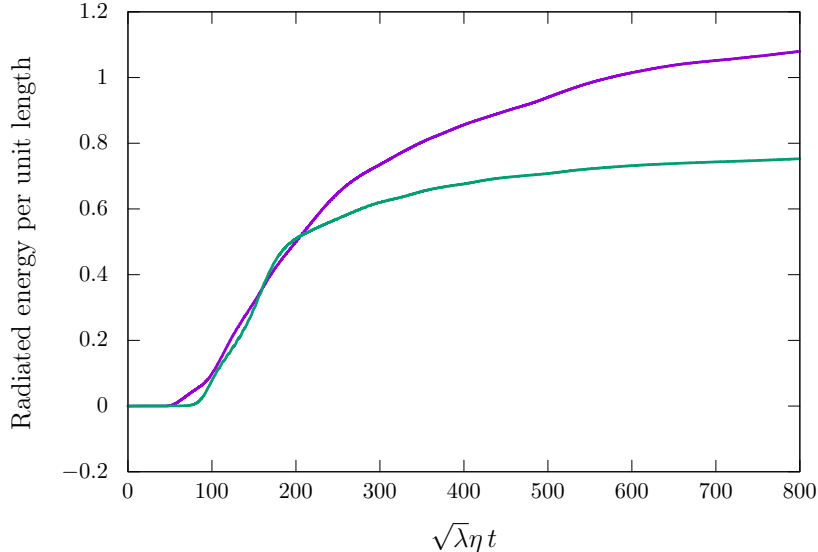


FIG. 4: Amount of energy radiated in the form of the massive mode (purple) and the massless mode (green) as a function of time. The quantity shown in the y axis is a dimensionless energy per unit length, namely, energy per unit length divided by η^2 . In this simulation, the shape mode is initialized homogeneously with amplitude $A(t=0) = 0.6$, which corresponds to an initial extra energy per unit length of 2.1 in these units.

the coupling of the zero mode to the massless Goldstone in the vacuum.

V. CONCLUSIONS

In this paper, we have shown that axionic strings can have parametric resonant effects due to the interaction between massless modes that parametrize the transverse motion of the string and the massive shape modes that modify the internal structure of the soliton. The presence of this instability leads to quantitative as well as qualitative differences in the spectrum of radiation from axionic strings. This makes this study interesting since it could have an effect in the estimate of axionic dark matter abundance from cosmological global string networks.

In order for this effect to become important, the strings must be in an excited state where part of the energy is stored in the shape mode. One of the instances where this can happen is, of course, during the formation of the strings. This has been studied in a $(2+1)d$ context in [34], where the results indicate that the amount of extra energy is not very relevant. However, it is important to remark that this conclusion may be different in a numerical simulation depending on the way one produces the initial conditions. Some of the lattice field theory simulations of these axionic strings use some period of relaxation

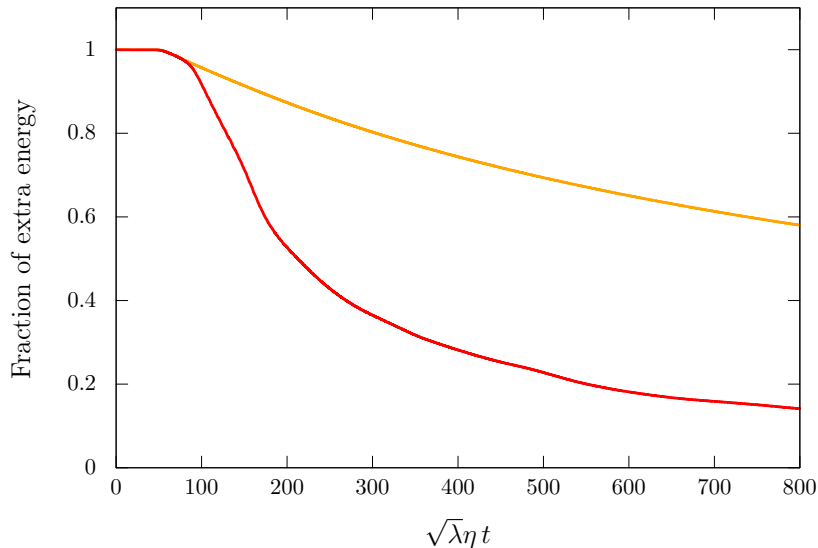


FIG. 5: Comparison of the extra energy for an excited string with the same initial amplitude of the shape mode but different size in the z direction. In orange we show the fraction of this initial energy in the case of an excited string where the parametric resonance is prevented by the short length in the z direction. In red, we show the case where the resonance is allowed and indeed it kicks in. Both these simulations use absorbing boundary conditions for the (x, y) boundaries of the box.

where these internal modes are presumably heavily suppressed. Others do not have this friction regime and could easily produce strings with an initial extra energy in these modes. Using our results in this paper, one can speculate that this would lead to a transient regime where massive as well as massless radiation would be efficiently produced from the network. In particular, some simulations have found a significant amount of massive radiation in the early stages of their evolution [24]. It would be interesting to understand whether this is due to the presence of these internal modes on the simulated strings and whether the instability we have discovered here is present.

Another way where this could be relevant is in the course of the network's evolution whenever strings intercommute. In those moments, it is likely that some of the energy could be absorbed by the string's internal modes. In fact, this has been the claim put forward in [48] based on the formation of loops from the intersection of long strings. Interestingly, this paper also shows that part of the spectrum of radiation from these loops is in the form of massive radiation, which would seem to be in agreement with our observations. It would be interesting to analyse these simulations in detail to identify whether or not there is any instability similar to the one presented in this paper.

The results we have obtained in this paper are quite similar to the parametric resonance in

domain wall strings found in [42]. We argued there that this effect could be encapsulated by adding to the effective action a term that represents the coupling of the scalar field describing the internal mode and the Ricci scalar of the string worldsheet. We conjecture that a similar term could be important for axionic strings and leave for future work to study the relevance of this term in an effective action for global strings which include a Nambu-Goto as well as a Kalb-Ramond terms.

Finally, it is clear that the mechanism that we described here would also be present in other field theory models with solitons where there are both types of excitation modes living on the worldvolume of the defects. In particular, it would be interesting to identify whether this can happen in the case of local strings or more generically in higher dimensional defects, like brane-like objects. We leave this for future investigations.

VI. ACKNOWLEDGEMENTS

We are grateful to Ken Olum, Tanmay Vachaspati, Alex Vilenkin and Giovanni Villadoro for many useful discussions and comments. This work is supported in part by the PID2021-123703NB-C21 grant funded by MCIN/AEI/10.13039/501100011033/ and by ERDF; “A way of making Europe”; by MCIN (project PID2020-113406GB-I00), the Basque Government grant (IT-1628-22) and the Basque Foundation for Science (IKERBASQUE). The numerical work carried out in this paper has been possible thanks to the computing infrastructure of the ARINA cluster at the University of the Basque Country (UPV/EHU).

Appendix A: Effective Lagrangian integrals

In this appendix we show explicitly the form of the space-dependent integrals in the effective Lagrangian (10). We impose the following normalization for the shape mode

$$\int_0^\infty r dr \eta_s^2(r) = 1. \quad (\text{A1})$$

The zero mode in the x -direction is decomposed as follows

$$\eta_0^x(r) = \eta_1(r) + \eta_2(r)e^{2i\theta}, \quad (\text{A2})$$

where

$$\eta_1(r) = \frac{1}{2} \left(f'(r) + \frac{f(r)}{r} \right), \quad \eta_2(r) = \frac{1}{2} \left(f'(r) - \frac{f(r)}{r} \right). \quad (\text{A3})$$

From the asymptotic form of $f(r)$, $f(r) = 1 - 1/r^2 + \mathcal{O}(1/r^4)$ it is easy to see that, for large r , the modulus of the zero mode grows as $1/r$, and as a consequence the zero mode is

not normalizable. This is the origin of the logarithmic divergences in (10). The convergent integrals are given by the following expressions

$$I_{A,3} = \int_0^\infty dr r f(r) \eta_s^3(r) \approx 0.197, \quad (\text{A4})$$

$$I_{A,4} = \frac{1}{4} \int_0^\infty dr r \eta_s^4(r) \approx 0.0188, \quad (\text{A5})$$

$$I_{D,4} = \frac{3}{32} \int_0^\infty dr r (\eta_1^4(r) + 4\eta_1^2(r)\eta_2^2(r) + \eta_2^4(r)) \approx 7.36 \times 10^{-4}, \quad (\text{A6})$$

$$I_{AD,3} = \int_0^\infty dr r \eta_s(r) (\eta_1^2(r) + \eta_1(r)\eta_2(r) + \eta_2^2(r)) \approx 0.0904, \quad (\text{A7})$$

$$I_{AD,4} = \frac{1}{2} \int_0^\infty dr r \eta_s^2(r) (\eta_1^2(r) + \eta_1(r)\eta_2(r) + \eta_2^2(r)) \approx 0.0185, \quad (\text{A8})$$

$$I_{D,2} = \int_0^\infty dr r \left(\frac{1}{2} f^2(r) (\eta_1^2(r) + \eta_1(r)\eta_2(r) + \eta_2^2(r)) + \frac{1}{2} (\eta_1'^2(r) + \eta_2'^2(r)) - \frac{1}{4} (\eta_1^2(r) + \eta_2^2(r)) + \frac{2}{r^2} \eta_2^2(r) \right) \approx -1.86 \times 10^{-4}. \quad (\text{A9})$$

The remaining, logarithmically divergent integral, has the form

$$I_D(R) = \frac{1}{2} \int_0^R dr r (\eta_1^2(r) + \eta_2^2(r)). \quad (\text{A10})$$

For $R = 40$, its numerical value is $I_D(40) \approx 0.806$.

As we pointed out in the main text, complete agreement in Fig. 3 is not obtained unless we slightly modify a few numbers involved in Eqs. (11). In the example we have shown, the required changes are the following:

- $I_{AD,3} \rightarrow 1.17 \times I_{AD,3}$
- $w_z^2 + I_{D,2}/I_D(R) \approx 0.207 \rightarrow 0.2077$

We attribute these imprecisions to the fact that all the functions involved in the integrals above are found numerically, and thus they come with some degree of uncertainty. The integral $I_{D,2}$ was found to be particularly sensitive to the number of points used for the integrand.

Appendix B: Implementation of our numerical lattice field theory simulations

In this appendix we provide the details of the lattice field theory simulations discussed in the main text. The simulations were run in a $3 + 1$ dimensional box with sides of

lengths L_x , L_y and L_z where the string lied along the z direction. The lattice spacing Δx was chosen to be the same in the three directions, so the total number of lattice points was $L_x \times L_y \times L_z / (\Delta x)^3$. Finally, Δt will denote the time step used in the simulations.

We solve the equations of motion employing the staggered leapfrog method and nearest neighbours for the discretization of the derivatives. Moreover, we implement Message Passing Interface (MPI) to handle the huge number of lattice points, which is typically of several million.

1. Dimensionless variables

In order to solve the equations of motion (2) in a discrete lattice, we first define the following dimensionless variables:

$$\tilde{x}^\mu = m_r x^\mu, \quad \tilde{L}_{x,y,z} = m_r L_{x,y,z}, \quad \tilde{\phi} = \phi/\eta, \quad (\text{B1})$$

where $m_r = \sqrt{\lambda\eta}$ is the mass of small fluctuations of the radial part of the field about the vacuum. With these redefinitions, the action reads

$$S = \frac{1}{\lambda} \int d^4 \tilde{x} \left[\partial_\mu \tilde{\phi}^* \partial^\mu \tilde{\phi} - \frac{1}{4} \left(\tilde{\phi}^* \tilde{\phi} - 1 \right)^2 \right] \quad (\text{B2})$$

and the equations of motion are free of parameters:

$$\partial_\mu \partial^\mu \tilde{\phi} + \frac{1}{2} \left(\tilde{\phi}^* \tilde{\phi} - 1 \right) \tilde{\phi} = 0, \quad (\text{B3})$$

where partial derivatives are now with respect to the dimensionless spacetime coordinates. These are the equations we solve in our simulations. In what follows, we will drop the tildes over the variables for the sake of simplicity in notation.

2. Boundary conditions

We employed periodic boundary conditions in the z direction (along which the string lies) and absorbing boundary conditions in the x and y directions. The latter were implemented by imposing the following condition at the boundaries, for every value of the z coordinate:

$$\frac{\partial \phi}{\partial t} + \frac{\partial \phi}{\partial x} \frac{x}{\sqrt{x^2 + y^2}} + \frac{\partial \phi}{\partial y} \frac{y}{\sqrt{x^2 + y^2}} \Big|_{x=\pm L_x/2, y=\pm L_y/2} = 0. \quad (\text{B4})$$

This condition is tailored to absorb radiation with radial incidence at the boundaries. Indeed, the idea behind this equation is to force the field to behave as an outgoing travelling wave

at the x, y boundaries. Far away from the string core, the real and imaginary parts of the field can be approximated by their vacuum expectation value plus a cylindrically symmetric travelling wave of the form

$$\xi(t, x, y) \propto \frac{1}{(x^2 + y^2)^{1/4}} \cos\left(k\sqrt{x^2 + y^2} - \beta t + \delta\right), \quad (\text{B5})$$

where k , β and δ are, respectively, the wave number, the angular frequency and the phase of the radiation. One can show that such a wave is a solution to Eq. (B4) if $k = \beta$, which means that the absorbing condition works better for massless radiation. However, massive radiation emitted by the string turned out to be efficiently absorbed as well.

3. Details of the simulations of section IV

For the simulation corresponding to Fig. 2 in section IV, where the amplification of the zero mode occurs, we chose $L_x = L_y = 80$ and $L_z = 40$, with lattice spacing $\Delta x = 0.2$ and time step $\Delta t = 0.1$. The static string solution was perturbed initially with the shape mode and a small amplitude zero mode in the x direction:

$$\phi(r, \theta, t = 0) = [f(r) + A(t = 0)\eta_s(r)]e^{i\theta} + D(t = 0)\sin(w_z z)\eta_x^0(r, \theta), \quad (\text{B6})$$

with $A(t = 0) = 0.5$, $D(t = 0) = 0.01$ and $\omega_z = 6\pi/L_z$.

For the comparison shown in Fig. 3 of the amplitudes of the modes with the solution of the coupled equations Eq. (11), we performed a different simulation with a smaller initial amplitude of the shape mode in order to reduce the effects of radiation as much as possible. In that case we chose $A(t = 0) = 0.1$, $D(t = 0) = 0.1$ and $w_z = 2\pi/L_z$, in a lattice with $L_x = L_y = 80$, $L_z = 13.8$, $\Delta x = 0.1$ and $\Delta t = 0.05$.

The projections needed to read the amplitude of the modes in the numerical simulations were computed as follows. Firstly, we assume that the field configuration at any time is given by

$$\phi(t, \mathbf{x}) = f(r)e^{i\theta} + A(t)\eta_s(r)e^{i\theta} + D(t)\eta_x^0(r, \theta)\cos(w_z z) + R(t, \mathbf{x}), \quad (\text{B7})$$

where $R(t, \mathbf{x})$ denotes collectively the scattering states. In order to find the amplitude of the shape mode, $A(t)$, we multiply both sides of Eq. (B7) by $\eta_s(r)e^{-i\theta}$ and integrate the real part over all space to get

$$A(t) = \frac{1}{2\pi L_z} \int_{-L_z/2}^{L_z/2} dz \int_0^{2\pi} d\theta \int_0^{r_{\max}} dr r [\phi_1(r, \theta, z, t)\cos\theta + \phi_2(r, \theta, z, t)\sin\theta] \eta_s(r), \quad (\text{B8})$$

where ϕ_1 and ϕ_2 are the real and imaginary parts of ϕ , respectively. Similarly, the amplitude of the zero mode can be obtained by projecting onto $(\eta_x^0)^*$. The result is

$$D(t) = \frac{2\pi \int_0^{L_z/2} dz \int_0^{2\pi} d\theta \int_0^{r_{\max}} dr r \left[\phi_1 \left(f' \cos^2 \theta + \frac{f}{r} \sin^2 \theta \right) + \phi_2 \left(f' - \frac{f}{r} \right) \sin \theta \cos \theta \right]}{L_z \int_0^{2\pi} d\theta \int_0^{r_{\max}} dr r \left[(f')^2 + \left(\frac{f}{r} \right)^2 \right]}. \quad (\text{B9})$$

Finally, in section IV A we compute the energy radiated by the string when the parametric resonance of the zero mode takes place (see Fig. 4). As mentioned in the main text, this is done by integrating the radiated power over the surface of a distant box surrounding the string. In order to account separately for the energy radiated in massive and massless modes, we follow the prescription given in [41, 46]. The 00 and 0*i* components of the energy-momentum tensor can be written as

$$T^{00} = \Pi_\varphi^2 + (\mathcal{D}\varphi)^2 + \Pi_\alpha^2 + (\mathcal{D}\alpha)^2 + V(\phi_1, \phi_2), \quad (\text{B10})$$

$$T^{0i} = 2 [\Pi_\varphi (\mathcal{D}\varphi)_i + \Pi_\alpha (\mathcal{D}\alpha)_i], \quad (\text{B11})$$

where

$$\Pi_\varphi = \frac{\phi_1 \partial_t \phi_1 + \phi_2 \partial_t \phi_2}{\sqrt{\phi_1^2 + \phi_2^2}}, \quad (\text{B12})$$

$$\mathcal{D}\varphi = \left(\frac{\phi_1 \partial_x \phi_1 + \phi_2 \partial_x \phi_2}{\sqrt{\phi_1^2 + \phi_2^2}}, \frac{\phi_1 \partial_y \phi_1 + \phi_2 \partial_y \phi_2}{\sqrt{\phi_1^2 + \phi_2^2}}, \frac{\phi_1 \partial_z \phi_1 + \phi_2 \partial_z \phi_2}{\sqrt{\phi_1^2 + \phi_2^2}} \right), \quad (\text{B13})$$

$$\Pi_\alpha = \frac{\phi_1 \partial_t \phi_2 - \phi_2 \partial_t \phi_1}{\sqrt{\phi_1^2 + \phi_2^2}}, \quad (\text{B14})$$

$$\mathcal{D}\alpha = \left(\frac{\phi_1 \partial_x \phi_2 - \phi_2 \partial_x \phi_1}{\sqrt{\phi_1^2 + \phi_2^2}}, \frac{\phi_1 \partial_y \phi_2 - \phi_2 \partial_y \phi_1}{\sqrt{\phi_1^2 + \phi_2^2}}, \frac{\phi_1 \partial_z \phi_2 - \phi_2 \partial_z \phi_1}{\sqrt{\phi_1^2 + \phi_2^2}} \right). \quad (\text{B15})$$

The terms with φ correspond to the contribution of the massive modes, while those with α are identified as the contribution of the massless modes. Therefore, their corresponding radiated powers are given by

$$P_{\text{massive}} = 2 \left[\int_{-L_z/2}^{L_z/2} dz \int_{-L_y/2}^{L_y/2} dy \left(\Pi_\varphi (\mathcal{D}\varphi)_1 \Big|_{x=-L_x/2} + \Pi_\varphi (\mathcal{D}\varphi)_1 \Big|_{x=L_x/2} \right) + \int_{-L_z/2}^{L_z/2} dz \int_{-L_x/2}^{L_x/2} dx \left(\Pi_\varphi (\mathcal{D}\varphi)_2 \Big|_{y=-L_y/2} + \Pi_\varphi (\mathcal{D}\varphi)_2 \Big|_{y=L_y/2} \right) \right], \quad (\text{B16})$$

$$P_{\text{massless}} = 2 \left[\int_{-L_z/2}^{L_z/2} dz \int_{-L_y/2}^{L_y/2} dy \left(\Pi_\alpha (\mathcal{D}\alpha)_1 \Big|_{x=-L_x/2} + \Pi_\alpha (\mathcal{D}\alpha)_1 \Big|_{x=L_x/2} \right) + \int_{-L_z/2}^{L_z/2} dz \int_{-L_x/2}^{L_x/2} dx \left(\Pi_\alpha (\mathcal{D}\alpha)_2 \Big|_{y=-L_y/2} + \Pi_\alpha (\mathcal{D}\alpha)_2 \Big|_{y=L_y/2} \right) \right]. \quad (\text{B17})$$

For the simulation corresponding to Fig. 4 we used $L_x = L_y = 80$, $L_z = 14$, $\Delta x = 0.1$ and $\Delta t = 0.05$. The initial amplitude of the shape mode was $A(t = 0) = 0.6$ in this case.

-
- [1] R. D. Peccei and H. R. Quinn, Phys. Rev. Lett. **38**, 1440 (1977).
 - [2] S. Weinberg, Phys. Rev. Lett. **40**, 223 (1978).
 - [3] F. Wilczek, Phys. Rev. Lett. **40**, 279 (1978).
 - [4] J. Preskill, M. B. Wise, and F. Wilczek, Physics Letters B **120**, 127 (1983), ISSN 0370-2693.
 - [5] L. Abbott and P. Sikivie, Physics Letters B **120**, 133 (1983), ISSN 0370-2693.
 - [6] M. Dine and W. Fischler, Physics Letters B **120**, 137 (1983), ISSN 0370-2693.
 - [7] T. W. B. Kibble, J. Phys. **A9**, 1387 (1976).
 - [8] A. Vilenkin and A. E. Everett, Phys. Rev. Lett. **48**, 1867 (1982).
 - [9] A. Vilenkin and T. Vachaspati, Phys. Rev. **D35**, 1138 (1987).
 - [10] M. Kawasaki, K. Saikawa, and T. Sekiguchi, Phys. Rev. D **91**, 065014 (2015), 1412.0789.
 - [11] P. Sikivie, Phys. Rev. Lett. **48**, 1156 (1982).
 - [12] C. Hagmann and P. Sikivie, Nucl. Phys. **B363**, 247 (1991).
 - [13] M. Yamaguchi, M. Kawasaki, and J. Yokoyama, Phys. Rev. Lett. **82**, 4578 (1999), hep-ph/9811311.
 - [14] C. Hagmann, S. Chang, and P. Sikivie, Phys. Rev. **D63**, 125018 (2001), hep-ph/0012361.
 - [15] M. Yamaguchi and J. Yokoyama, Phys. Rev. D **67**, 103514 (2003), hep-ph/0210343.
 - [16] L. Fleury and G. D. Moore, JCAP **1601**, 004 (2016), 1509.00026.
 - [17] L. M. Fleury and G. D. Moore, JCAP **1605**, 005 (2016), 1602.04818.
 - [18] V. B. Klaer and G. D. Moore, JCAP **1710**, 043 (2017), 1707.05566.
 - [19] M. Kawasaki, T. Sekiguchi, M. Yamaguchi, and J. Yokoyama, PTEP **2018**, 091E01 (2018), 1806.05566.
 - [20] M. Gorghetto, E. Hardy, and G. Villadoro, JHEP **07**, 151 (2018), 1806.04677.
 - [21] A. Vaquero, J. Redondo, and J. Stadler (2018), [JCAP1904,012(2019)], 1809.09241.
 - [22] C. J. A. P. Martins, Phys. Lett. B **788**, 147 (2019), 1811.12678.
 - [23] M. Hindmarsh, J. Lizarraga, A. Lopez-Eiguren, and J. Urrestilla, Phys. Rev. Lett. **124**, 021301 (2020), 1908.03522.
 - [24] M. Gorghetto, E. Hardy, and G. Villadoro, SciPost Phys. **10**, 050 (2021), 2007.04990.
 - [25] M. Hindmarsh, J. Lizarraga, A. Lopez-Eiguren, and J. Urrestilla, Phys. Rev. D **103**, 103534 (2021), 2102.07723.
 - [26] M. Hindmarsh, J. Lizarraga, A. Lopez-Eiguren, and J. Urrestilla (2021), 2109.09679.
 - [27] M. Buschmann, J. W. Foster, A. Hook, A. Peterson, D. E. Willcox, W. Zhang, and B. R.

- Safdi, *Nature Commun.* **13**, 1049 (2022), 2108.05368.
- [28] H. Arodz, *Acta Phys. Polon.* **B22**, 511 (1991).
 - [29] M. Goodband and M. Hindmarsh, *Phys. Rev.* **D52**, 4621 (1995).
 - [30] T. Kojo, H. Suganuma, and K. Tsumura, *Phys. Rev.* **D75**, 105015 (2007), hep-ph/0702014.
 - [31] A. Alonso-Izquierdo, W. Garcia Fuertes, and J. Mateos Guilarte, *Phys. Lett.* **B753**, 29 (2016), 1509.06632.
 - [32] A. Alonso-Izquierdo, W. Garcia Fuertes, and J. Mateos Guilarte, *JHEP* **05**, 074 (2016), 1602.09084.
 - [33] J. J. Blanco-Pillado, D. Jiménez-Aguilar, and J. Urrestilla, *JCAP* **01**, 027 (2021), 2006.13255.
 - [34] J. J. Blanco-Pillado, D. Jiménez-Aguilar, J. M. Queiruga, and J. Urrestilla, *JCAP* **10**, 047 (2021), 2107.02215.
 - [35] N. S. Manton and H. Merabet, *Nonlinearity* **10**, 3 (1997), hep-th/9605038.
 - [36] D. Garfinkle and T. Vachaspati, *Phys. Rev. D* **37**, 257 (1988).
 - [37] R. L. Davis and E. P. S. Shellard, *Phys. Lett. B* **214**, 219 (1988).
 - [38] A. Dabholkar and J. M. Quashnock, *Nucl. Phys. B* **333**, 815 (1990).
 - [39] R. A. Battye and E. P. S. Shellard, *Nucl. Phys.* **B423**, 260 (1994), astro-ph/9311017.
 - [40] R. A. Battye and E. P. S. Shellard, *Phys. Rev.* **D53**, 1811 (1996), hep-ph/9508301.
 - [41] A. Drew and E. P. S. Shellard, *Phys. Rev. D* **105**, 063517 (2022), 1910.01718.
 - [42] J. J. Blanco-Pillado, D. Jiménez-Aguilar, J. M. Queiruga, and J. Urrestilla (2022), 2209.12945.
 - [43] M. Kalb and P. Ramond, *Phys. Rev. D* **9**, 2273 (1974).
 - [44] Vachaspati and T. Vachaspati, *Phys. Lett. B* **238**, 41 (1990).
 - [45] I. Kovacic, R. Rand, and S. Mohamed Sah, *Applied Mechanics Reviews* **70** (2018).
 - [46] A. Drew and E. P. S. Shellard (2022), 2211.10184.
 - [47] K. D. Olum and J. J. Blanco-Pillado, *Phys. Rev. Lett.* **84**, 4288 (2000), astro-ph/9910354.
 - [48] A. Saurabh, T. Vachaspati, and L. Pogosian, *Phys. Rev. D* **101**, 083522 (2020), 2001.01030.